Electrochemical properties of monolithic nickel sulfide electrodes for use in sodium batteries

Dae-Yeon Go [a], Jinsoo Park [b,**], Pan-Jin Noh [a], Gyu-Bong Cho [a], Ho-Suk Ryu [a], Tae-Hyeon Nam [a], Hyo-Jun Ahn [a], Ki-Won Kim [a,*]

[a] Department of Materials Engineering and Convergence Technology, RIGET, Gyeongsang National University, 501 Jinju-Daero, Jinju, Gyeongnam 660-701, South Korea
[b] Department of Materials and Energy Engineering, Kyungwoon University, 730 Gangdong-ro, Sandong-meon, Gumi-si, Gyeongbuk 730-739, South Korea

ARTICLE INFO

ABSTRACT

Monolithic nickel sulfide electrodes were prepared using a facile synthesis method, sulfuration and annealing. As-prepared Ni_3S_2 electrodes were characterized by X-ray diffractometry and field emission scanning electron microscopy. Thermal stability was determined by thermal gravimetric analysis and differential scanning calorimetry. Electrochemical properties were measured by galvanostatic charge and discharge cycling for Na-ion batteries. Three kinds of Ni_3S_2 electrodes were prepared by varying the sulfuration time (5, 15 and 25 min). The electrochemical results indicated that the capacities increased with an increase in sulfuration time and the cycle performance was stable as a result of monolithic integration of nanostructured Ni_3S_2 on Ni plates, leading to low interfacial resistance.

© 2014 Elsevier Ltd. All rights reserved.

1. Introduction

Fossil fuel consumption has increased greenhouse gas emissions in the atmosphere, causing serious environmental problems such as global warming and pollution. There is an urgent need to develop alternative power sources such as solar and wind powers, which are called green energies. However, the energy supply generated from renewable sources is inconsistent and unpredictable. To secure an alternative energy supply, it is necessary to develop rechargeable batteries that can store and release energy on demand.

Currently available lithium ion batteries that use lithium metal oxide ($LiMO_2$, M = Co, Mn, Ni) and graphite can offer high power, high energy density, cycle life, and high rate capability to small mobile devices [1–3], but are limited when it comes to new emerging applications such as electrical energy storage systems (ESS), electric vehicles (EVs), and hybrid electric vehicles (HEVs), because of cost and safety. Instead, a wide range of metal sulfides has been proposed as candidates for cathode materials that provide high theoretical capacities at low cost [4–6]. Among the metal sulfides, nickel sulfide has the advantages of good electronic conductivity, environment-friendly, low cost, and high energy

capacity. Nickel sulfide is a material with a multiphase such as Ni_3S_2, $Ni_{3+x}S_2$, Ni_4S_{3+x}, Ni_6S_5, and Ni_7S_6. Among these phases Ni_3S_2 is electrochemically active, chemically stable, and compatible with organic solvents [4,7].

Traditionally, bulk Ni_3S_2 produced by ball-milling is contaminated and has low crystallinity [8]. A high-purity and nano-structured Ni_3S_2 can be synthesized through a variety of methods such as H_2S gas reacting with nickel nano-particles on graphene or the soft solution chemical route [9,10].

In this study, a facile method was employed to prepare nanostructured Ni_3S_2 on a nickel plate [11]. As some authors have proposed, it is expected that the synthesis of materials with an integrated nanostructure will have high surface areas and good ionic conductivity, as well as the benefits of not having a binder or conductive agent [12–14]. Monolithically integrated Ni_3S_2 on Ni plates was characterized using field emission electron microscopy (FE-SEM) and X-ray diffractometry (XRD). Thermal analysis was conducted to measure weight loss and phase transition temperature. Electrochemical measurements of monolithic Ni_3S_2 electrodes were taken for sodium ion batteries.

2. Experimental

Nickel (Ni) plates were polished to remove oxidation layers before the sulfuration process. For nickel sulfuration, a solution was prepared by adding sulfur (S, Sigma–Aldrich) to ammonium sulfide (($NH_4)_2S_x$, Kanto Chemical). Ni plates were soaked in the

* Corresponding author. Tel.: +82 55 772 1663; fax: +82 55 772 2586.
** Corresponding author. Tel.: +82 54 479 1153; fax: +82 54 479 1029.
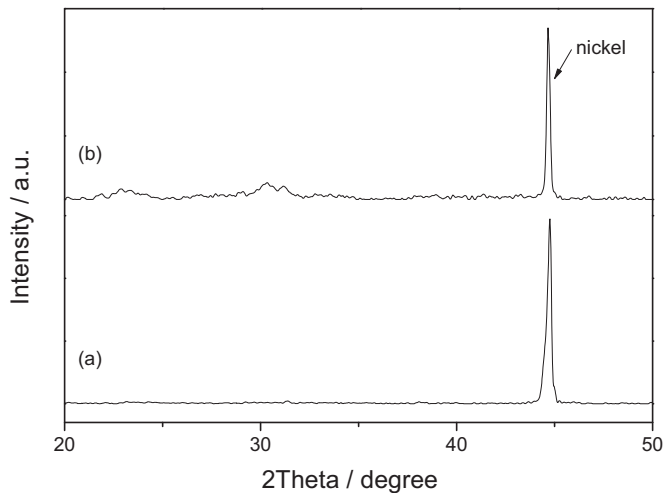E-mail addresses: jsp@ikw.ac.kr (J. Park), kiwonkim@gnu.ac.kr (K.-W. Kim).

Fig. 1. XRD patterns of (a) a bare nickel plate after being polished; and (b) a nickel plate after undergoing sulfuration for 25 min.

solution, which was heated up to 70 °C. Sulfuration proceeded for durations of 5 min, 15 min, and 25 min. The decolorized nickel plates were removed promptly from the solution, washed with ethanol, and then dried in an oven for 24 h. The sulfurated nickel plates were annealed at 500 °C for 3 h.

The as-prepared nickel sulfide plates were analyzed by thermal gravimetric analysis (TGA) and differential scanning calorimetry (DSC) under an Ar atmosphere using a thermal analyzer (Q600).
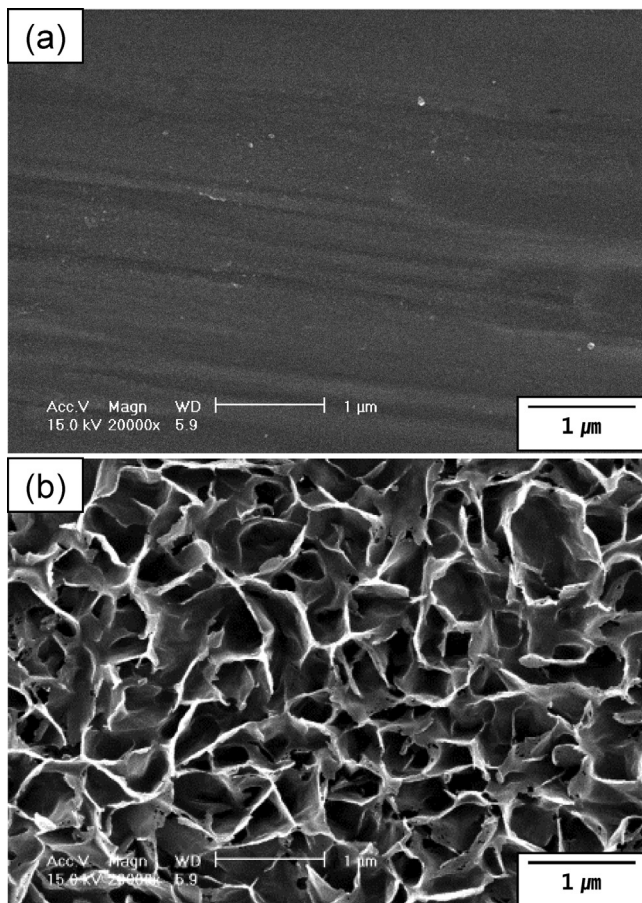

Fig. 2. FE-SEM images of (a) a bare nickel plate after being polished; and (b) a nickel plate after undergoing sulfuration for 25 min.
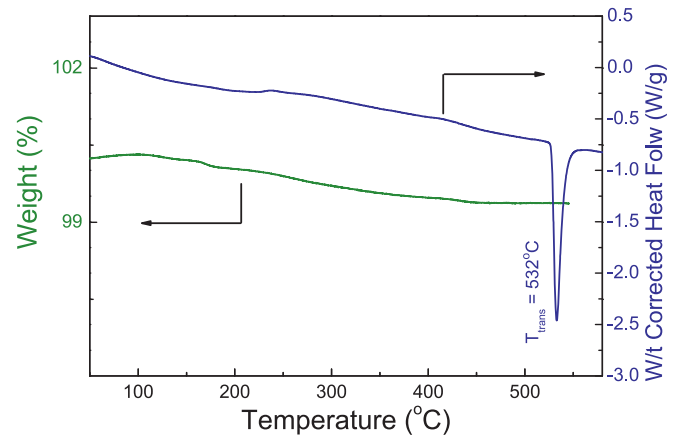

Fig. 3. TGA/DSC curves of an as-prepared nickel plate by sulfuration.

The temperature was ramped at a rate of 10 °C/min up to 550 °C and 600 °C for TGA and DSC, respectively. The crystallographic structure was confirmed by X-ray diffractometry (XRD, D3 Advance, Bruker) with a Cu X-ray tube. XRD patterns were recorded in the range of 20–50° at a scan speed of 1°/min. The morphologies were photographed using a field emission scanning electron microscope (FE-SEM, Philips XL30S FEG) with an acceleration voltage of 30 kV.

Two-electrode Swagelok-type cells were assembled by stacking sliced sodium metal (Na, Aldrich), a separator (Cellgard®-2400) with a liquid electrolyte, and the nickel sulfide electrode. The liquid electrolyte was 1 M sodium tetrafluoroborate salt (NaBF$_4$, Aldrich) dissolved in tetra ethylene glycol dimethyl ether (TEGDME, Aldrich). The whole cell assembly procedure was carried out in a glove box in a sophisticatedly controlled argon atmosphere because Na metal is extremely sensitive to oxygen and moisture. The charge/discharge cycling test was performed in the potential range of 0.5–2.5 V at room temperature using a WBCS 3000 battery tester (WonA Tech).

3. Results and discussion

Fig. 1 presents X-ray diffraction patterns of bare and sulfurated Ni plates. Both patterns show a sharp peak at 44.5°, corresponding
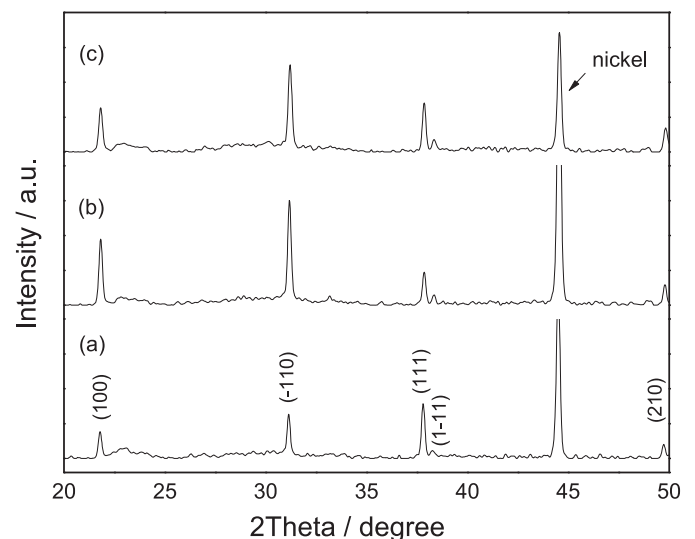

Fig. 4. XRD patterns of as-prepared Ni$_3$S$_2$ electrodes by sulfuration of nickel plates after heat treatment at 500 °C for 3 h: (a) for 5 min, (b) for 15 min, (c) for 25 min.
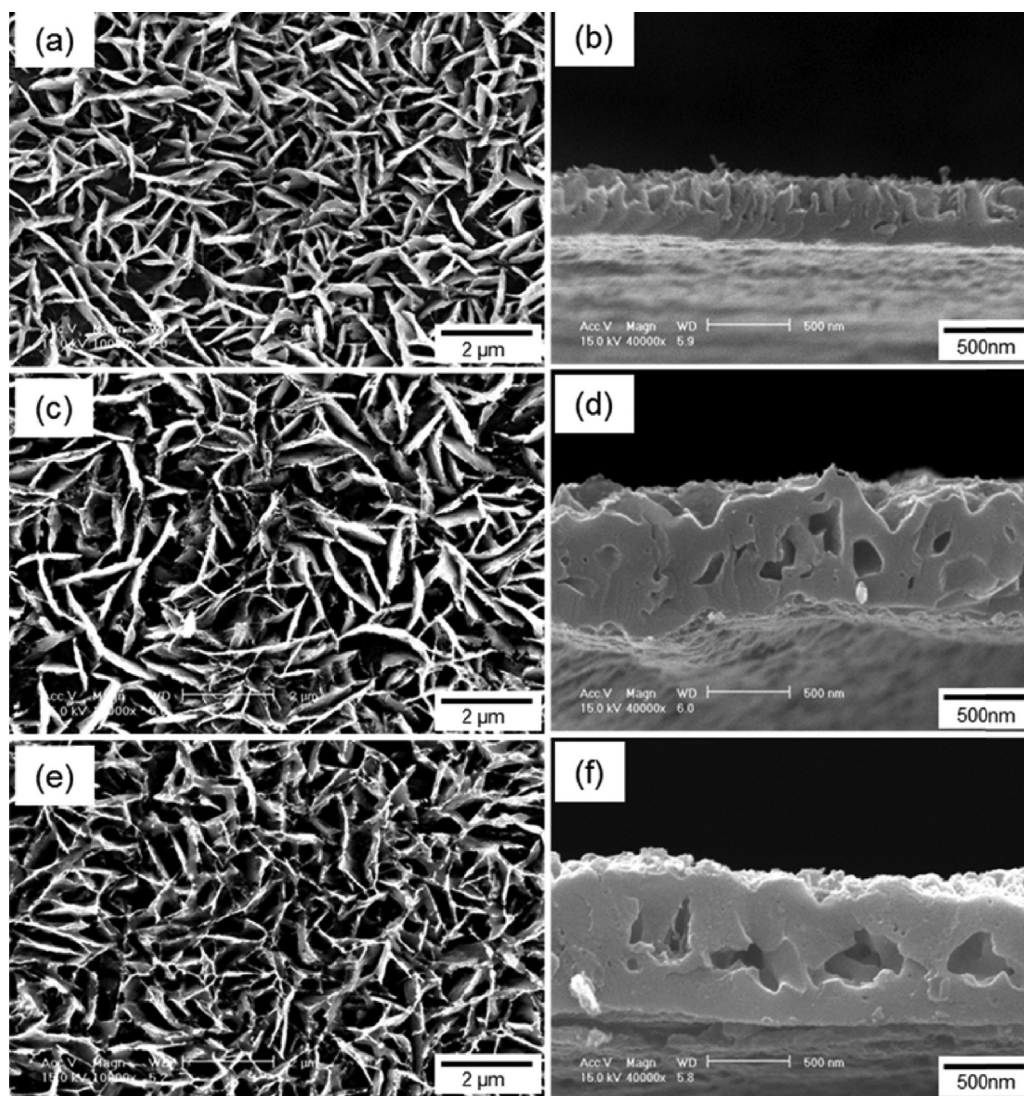
Fig. 5. Surface images of Ni plates with sulfuration of (a) 5 min, (c) 15 min and (e) 25 min after heat treatment at 500 °C for 3 h; and their corresponding cross-sectional images (b), (d) and (f).

to the (1 1 1) plain in the Ni cubic structure (JCPDS Card no. 87-0712). After sulfuration of Ni, two very broad peaks were observed at approximately 25° and 30°. Nickel-based compounds such as NiS, NiS_2, and Ni_3S_2 and sulfur lie in these 2 theta ranges. The pattern (b) of the sulfurated Ni plate indicates the sulfuration process can produce nickel sulfide compounds through a simple bath for a short time.

As shown in Fig. 2(a), the bare Ni plate has a smooth surface but after soaking in the sulfuration solution, the Ni surface was transformed into the monolithic dense petal garden seen in Fig. 2(b). Observation by FE-SEM confirms that Ni and S reacted in the ammonium sulfide solution. The monolithic petals on the Ni surface have a thickness of approximately 20 nm. These monolithically integrated petals attract great attention as they are formed during the facile process.

According to the nickel and sulfur phase diagram, the nickel sulfide composition varies along with the sulfur atomic percentage. Under moderate temperature conditions, the following phases can exist: NiS_2, Ni_3S_4, NiS, Ni_7S_6, and Ni_3S_2 in the order of sulfur content (high to low). In XRD and FE-SEM characterization, we could not obtain the stoichiometric ratio of Ni and S. Due to the reaction occurring at 70 °C, multiphase NiS_x was formed on the plate. Thermal analysis was employed to determine the weight loss

and phase transition temperature of the sulfurated Ni plate. Fig. 3 presents the thermal analysis using TGA and DSC. The weight loss measured by TGA (marked with an arrow on the left) was less than 1% up to 550 °C. This small weight loss can be attributed to evaporation of sulfur on the plate, which was not removed by drying. For DSC (marked with an arrow on the right), heat flow has a sharp peak at 532 °C, which is very close to the transition temperature (T_{trans}) of Ni_3S_2 and Ni_7S_6. Hence, it confirms the nickel sulfide phase contains 40–45% sulfur.

To obtain a high crystalline structure of nickel sulfide (Ni_3S_2), the as-prepared nickel plates were annealed at 500 °C. Above this temperature, the petal structure can break due to crystalline growth. Three Ni plates were sulfurated at different durations of 5 min, 15 min, and 25 min and heat-treated at 500 °C for 3 h under an Ar atmosphere. Fig. 4(a) shows the XRD patterns of three heat-treated samples. All the patterns had identical peak positions, which are readily indexed to heazlewoodite, Ni_3S_2 with a rhombohedral structure (JCPDS Card no. 85-1802). The intensities of Ni_3S_2 sulfurated for 15 min and 25 min are higher than for 5 min because the longer sulfuration time results in a thicker layer of nickel sulfide. The phase transition from amorphous to crystalline may cause a morphological change in the petal structure because it can accompany crystal growth. FE-SEM images for annealed samples
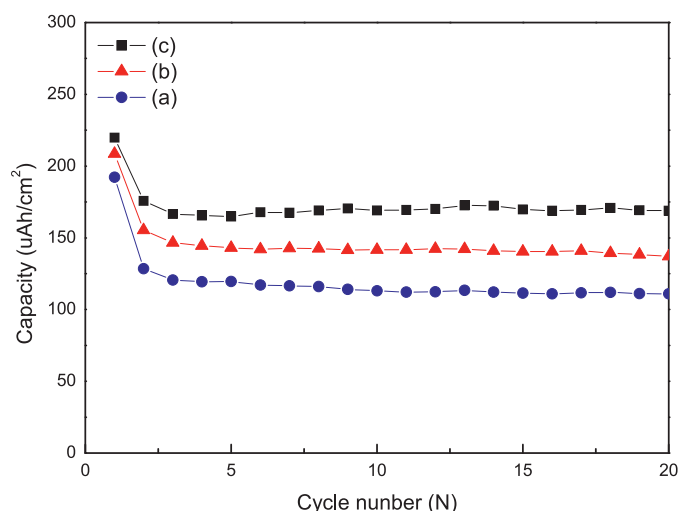
Fig. 6. Cycle lives of Na/Ni$_3$S$_2$ cells using nickel sulfide electrodes prepared by sulfuration for (a) 5 min, (b) 15 min, and (c) 25 min and heat-treated at 500 °C for 3 h.

Fig. 8. Nyquist plots of (a) a powder nickel sulfide electrode, (b) a monolithic nickel sulfide electrode.

are shown in Fig. 5. As one may notice, petals became thicker after heat treatment, but destruction of the structure due to abnormal growth was not observed. Cross-sectional images showed that thickness increased from 5 min to 15 min. After 25 min there was no change in thickness but the layer seemed to be denser.

Fig. 6 shows the cycle performances of Na/Ni$_3$S$_2$ cells to compare the three annealed nickel sulfides with monolithic petal structures. The current density applied to the cells was 20 µA/cm^2. As the sulfuration time increases from 5 to 25 min, monolithic Ni$_3$S$_2$ tends to have a higher capacity. The three samples delivered 193, 209 and 220 µA h/cm^2 at the first discharge and 129, 156 and 175 µA h/cm^2 at the second discharge, respectively. From the second discharge, Na/Ni$_3$S$_2$ cells show good cycling performance.

Fig. 7 shows the galvanostatic charge and discharge profiles for Ni$_3$S$_2$ sulfurated for 25 min. At the first discharge, the curve runs down forming two plateaus at the potential of 1.08 V and 0.93 V. At the second cycle, the plateau potential shifts to 1.05 V due to resistance variation in the cell. However, the discharge and charge behavior did not vary after successive cycling and displays stable discharge and charge capacities.

To compare monolithic Ni$_3$S$_2$ and bulk Ni$_3$S$_2$ powders, electrochemical impedance spectroscopy (EIS) was carried out

after the initial discharge. Nyquist plots are shown in Fig. 8. The monolithic Ni$_3$S$_2$ electrode has a lower interfacial resistance (R_{intf}) of 79 Ω than the bulk Ni$_3$S$_2$ powder electrode (122 Ω), which indicates that monolithic petal structures allow Na$^+$ in the electrolyte to move easily and increase the charge exchange rate at the interface. The low R_{intf} preferentially benefits the transfer rate of Na ions between the cathode and anode. Therefore, the good cycle performances of the Ni$_3$S$_2$ electrodes in Fig. 6 are due to the low interfacial resistance.

4. Conclusion

In this study, monolithic Ni$_3$S$_2$ electrodes were synthesized using the facile sulfuration method and annealing. As-prepared electrodes had a monolithically integrated petal structure on the Ni plate. Electrochemical properties showed that monolithic Ni$_3$S$_2$ had a lower interfacial resistance and stable operation without capacity decay. For the Ni$_3$S$_2$ sulfurated for 25 min, the initial discharge capacity was 220 µA h/cm^2. From characterization and electrochemical measurements, sulfuration is confirmed as a facile and effective method to develop high-performance electrodes with nanostructures monolithically integrated into the substrate for Na-ion batteries.
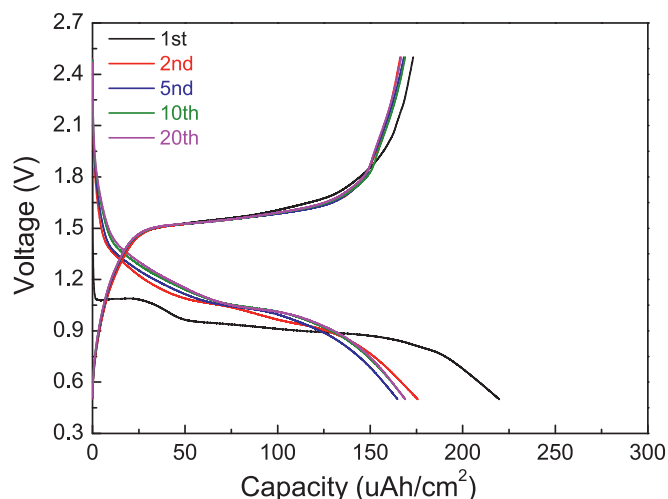
Fig. 7. Charge/discharge profiles of a Na/Ni$_3$S$_2$ cell using a nickel sulfide electrode prepared by sulfuration for 25 min and heat-treated at 500 °C for 3 h.
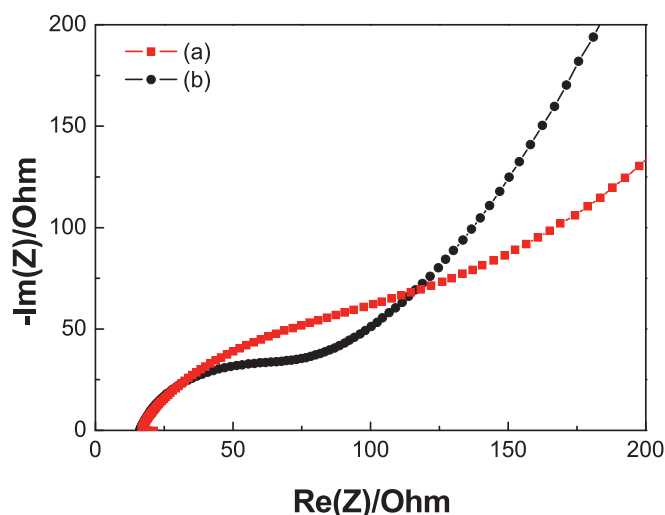
References

[1] Jia-Zhao Wang, Shu-Lei Chou, Sau-Yen Chew, Jia-Zeng Sun, Maria Forsyth, Douglas R. MacFarlane, Hua-Kun Liu, Nickel sulfide cathode in combination with an ionic liquid-based electrolyte for rechargeable lithium batteries, Solid State Ionics 179 (2008) 2379–2382.
[2] Jong-seon Kim, Sang-Won Lee, Xiaojing Liu, Gyu-Bong Cho, Ki-Won Kim, In-Shup Ahn, Jou-Hyeon Ahn, Guoxiu Wang, Hyo-Jun Ahn, Electrochemical properties of Na/Ni$_3$S$_2$ cells with liquid electrolytes using various sodium salts, Curr. Appl. Phys. 11 (2011) S11–S14.
[3] Jong-seon Kim, Gyu-Bong Cho, Ki-Won Kim, Jou-Hyeon Ahn, Guoxiu Wang, Hyo-Jun Ahn, The addition of iron to Ni$_3$S$_2$ electrode for sodium secondary battery, Curr. Appl. Phys. 11 (2011) S215–S218.

[4] Sang-Cheol Han, Hyun-Seok Kim, Min-sang Song, Jai-Young Paul S. Lee, Hyo-Jun Lee, Electrochemical properties of NiS as a cathode material for rechargeable lithium batteries prepared by mechanical alloying, J. Alloys Compd. 349 (2003) 290–296.

[5] F. Wu, H.X. Yang, Green Secondary Batteries, Science Press, Beijing, 2009.

[6] X.J. Liu, Z.Z. Xu, H.J. Ahn, S.K. Lyu, I.S. Ahn, Electrochemical characteristics of cathode materials NiS_2 and Fe-doped NiS_2 synthesized by mechanical alloying for lithium-ion batteries, Powder Technol. 229 (2012) 24–29.

[7] Jong-seon Kim, Hyo-Jun Ahn, Ho-Suk Ryu, Dong-Ju Kim, Gyu-Bong Cho, Ki-Won Kim, Tae-Hyeon Nam, Jou-Hyeon Ahn, The discharge properties of Na/Ni_3S_2 cell at ambient temperature, J. Power Sources 178 (2008) 852–856.

[8] Xiujian Zhu, Zhaoyin Wen, Zhonghua Gu, Shahua Huang, Room-temperature mechanosynthesis of Ni_3S_2 as cathode material for rechargeable lithium polymer batteries, J. Electrochem. Soc. 153 (2006) A504–A507.

[9] R.D. Tilley, D.A. Jefferson, The synthesis of nickel sulfide nanoparticles on graphitized carbon supports, J. Phys. Chem. B 106 (2002) 10895.

[10] S.H. Yu, M. Yoshimura, Fabrication of powders and thin films of various nickel sulfides by soft solution-processing routes, Adv. Mater. 12 (2002) 277.

[11] Yong-Chul Jung, Se-Young An, Sang-Hee Suh, Duck-Kyun Choi, Jin-Sang Kim, Ammonium sulfide treatment of HgCdTe substrate and its effects on electrical properties of ZnS/HgCdTe heterostructure, Thin Solid Films 483 (2005) 407–410.

[12] Chong Wang, Dianlong Wang, Qiuming Wang, Wang Lin, Fabrication of three-dimensional porous structured Co_3O_4 and its application in lithium-ion batteries, Eletrochim. Acta 55 (2010) 6420–6425.

[13] Shichao Zhang, Yalan Xing, Tao Jiang, Zhijia Du, Feng Li, He Lei, Wenbo Liu, A three-dimensional tin-coated nanoporous copper for lithium-ion battery anodes, J. Power Sources 196 (2011) 6915–6919.

[14] P. Zhang, Z.P. Guo, S.G. Kang, Y.J. Choi, C.J. Kim, K.W. Kim, H.K. Liu, Three-dimensional Li_2O–NiO–CoO composite thin-film anode with network structure for lithium-ion batteries, J. Power Sources 189 (2009) 566–570.